Supporting Information

Effect of Large Dimensional Deformation of Porous Structure on Stem Cell Fate Activated by Poly(L-glutamic acid)-Based Shape Memory Scaffolds

Weijun Zhang[a], Kunxi Zhang[a]*, Guifei Li[a], Shifeng Yan[a], Lei Cui[b], and Jingbo Yin[a]*

a Department of Polymer Materials, Shanghai University, 99 Shangda Road, Shanghai 200444, P. R. China. E-mail: zhangkunxi@shu.edu.cn; jbyin@oa.shu.edu.cn

b Department of Orthopaedics Surgery, Shanghai Tongji Hospital, Tongji University School of Medicine, 389 Xincun Road, Shanghai 200065, P. R. China.

* Corresponding author: Dr. Kunxi Zhang

E-mail: zhangkunxi@shu.edu.cn

* Corresponding author: Prof. Jingbo Yin

E-mail: jbyin@oa.shu.edu.cn

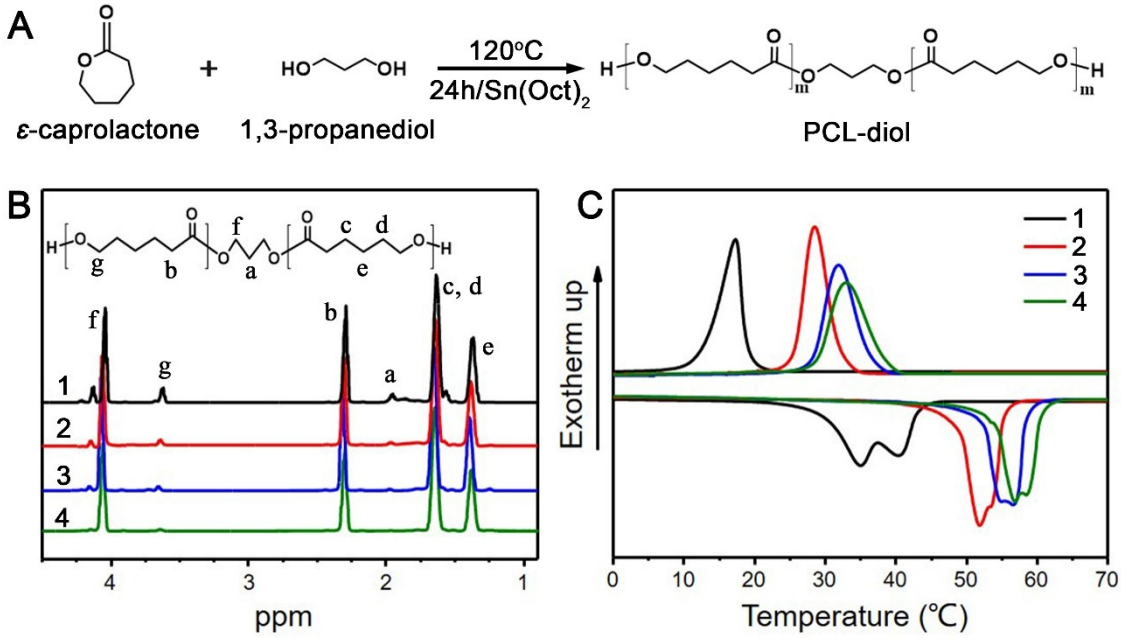

Figure S1. Characterization of PCL-diols. (A) The synthesis route of PCL-diol. (B) ^{1}H NMR spectrums and (C) DSC curves of PCL-diols with four different molecular weight: (1) 1102; (2) 3496; (3) 7144; (4) 11476.

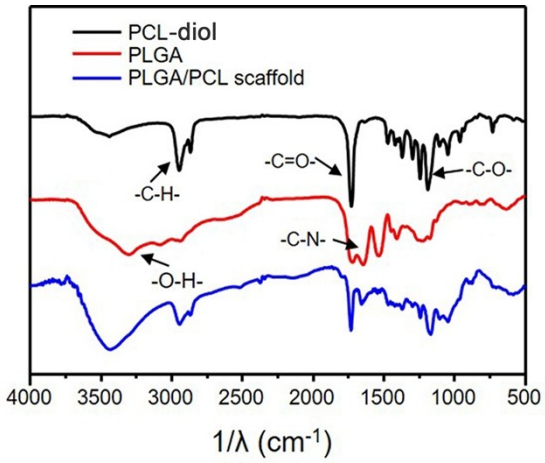

Figure S2. (A) FTIR spectrum of PCL-diol, PLGA and PLGA/PCL scaffold.

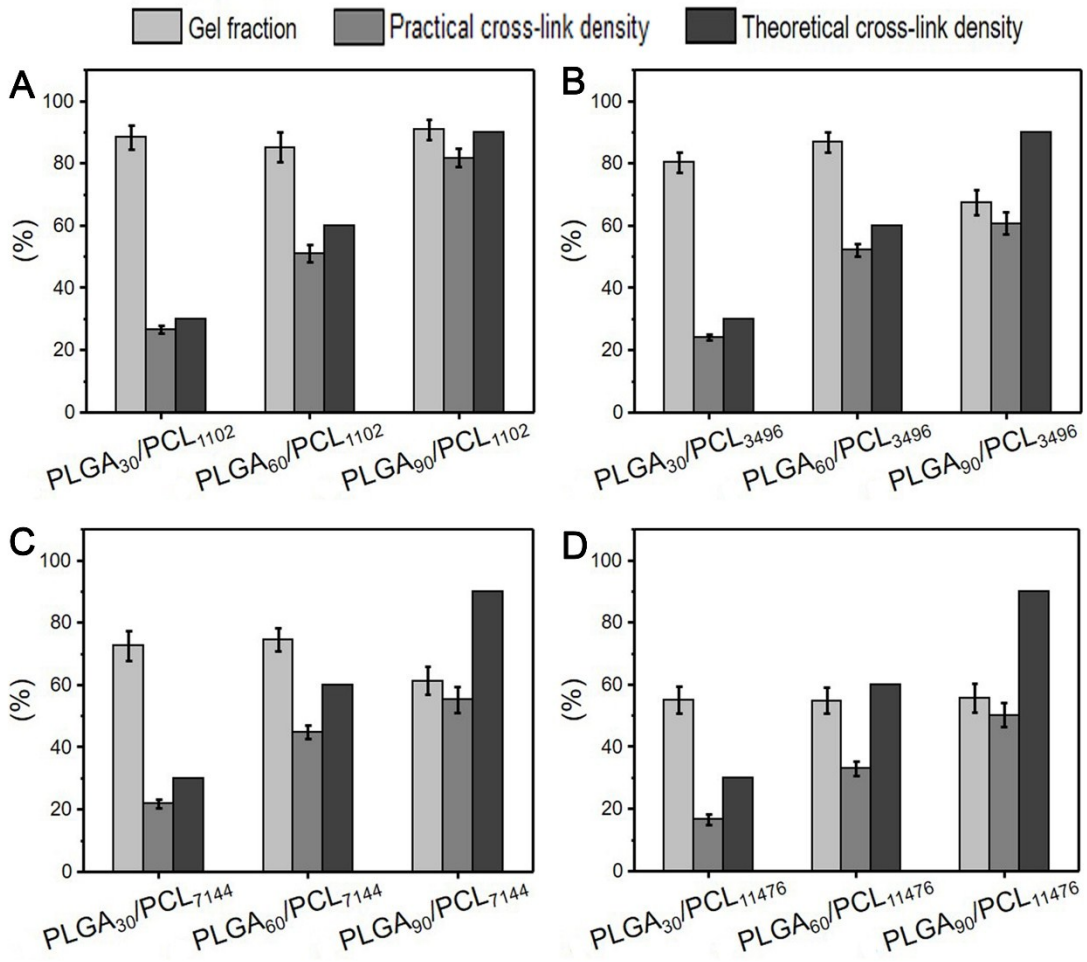

Figure S3. Gel fraction and cross-link density of $PLGA_x/PCL_y$ scaffolds where x and y represent theoretical cross-link density and PCL-diol molecular weight, respectively. (A) $PLGA_{30,60,90}/PCL_{1102}$. (B) $PLGA_{30,60,90}/PCL_{3496}$. (C) $PLGA_{30,60,90}/PCL_{7144}$. (D) $PLGA_{30,60,90}/PCL_{11476}$.

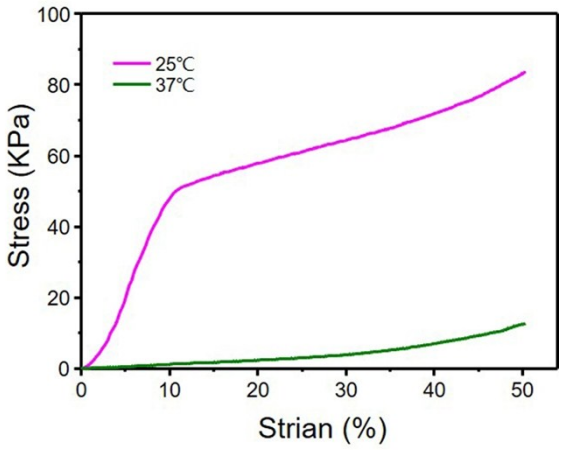

Figure S4. Stress-strain curves of $PLGA_{60}/PCL_{3496}$ scaffolds at 25 °C and 37 °C. **Response #1.5**

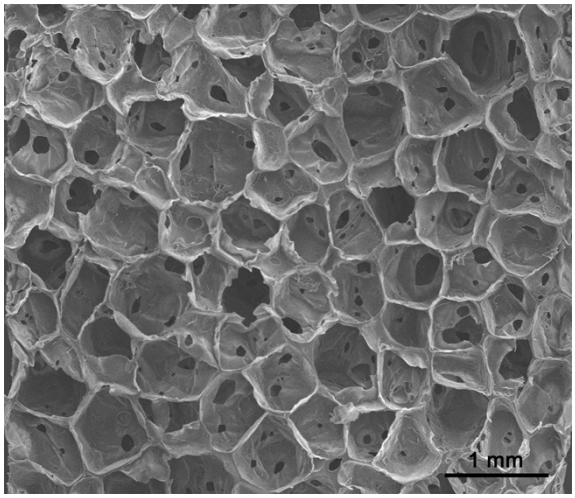

Figure S5. Porous structure of $PLGA_{60}/PCL_{3496}$ scaffolds.

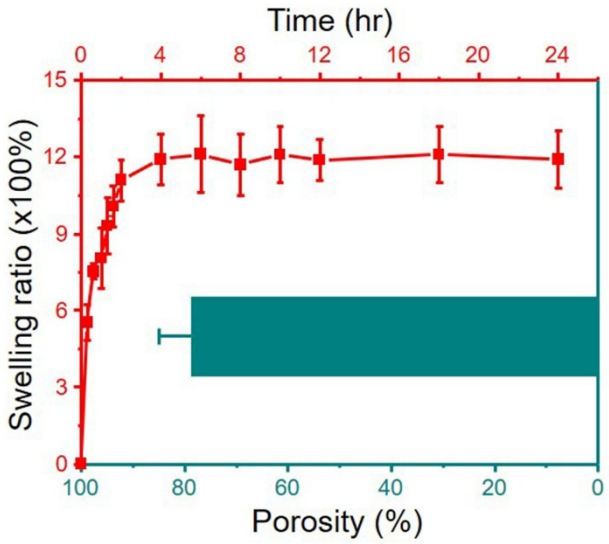

Figure S6. Swelling ratio and porosity of $PLGA_{60}/PCL_{3496}$ scaffolds.

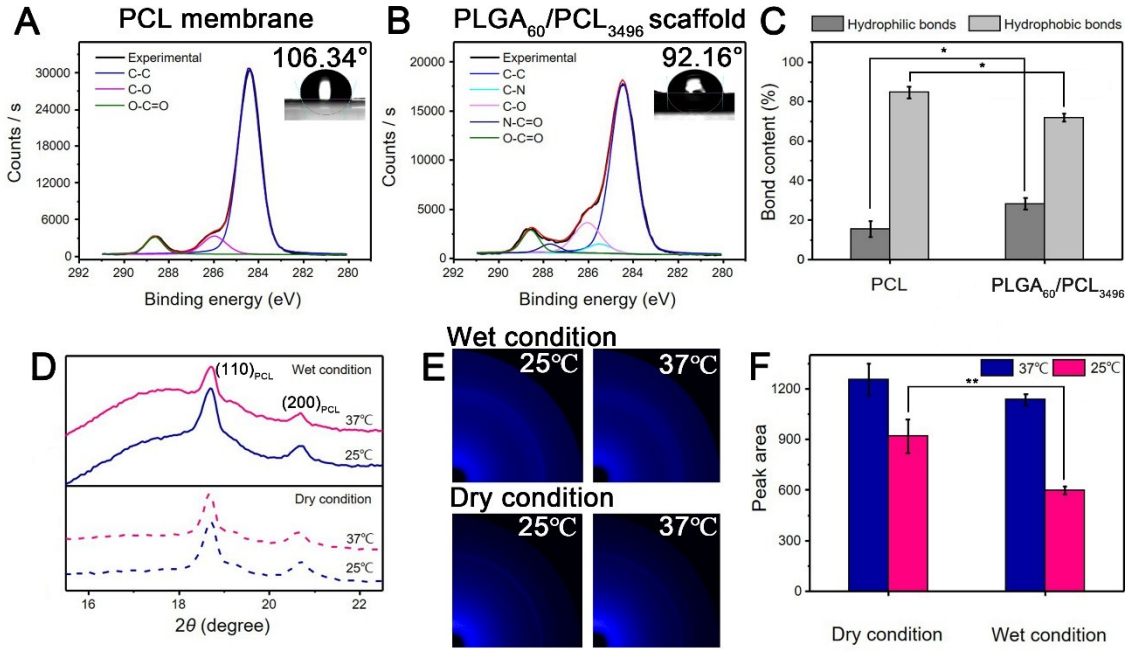

Figure S7. Hydrophilicity of $PLGA_{60}/PCL_{3496}$ porous scaffolds. XPS C 1s spectra and contact angle of (A) PCL membrane and (B) $PLGA_{60}/PCL_{3496}$ porous scaffold surface. Illustration is the contact angle of each material. (C) Proportion of hydrophilic and hydrophobic bonds on the PCL membrane and $PLGA_{60}/PCL_{3496}$ porous scaffold surface. (D) One-dimensional WAXS intensity profiles of dry and wet $PLGA_{60}/PCL_{3496}$ porous scaffolds, (E) corresponding WAXS patterns and (F) peak area at 25 °C and 37 °C. $*P < 0.05$. $**P < 0.01$.

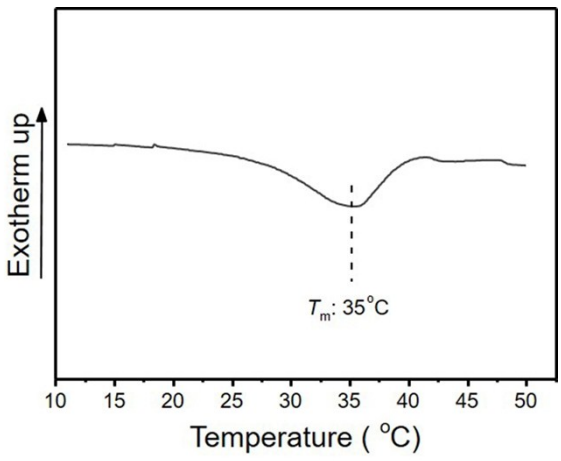

Figure S8. DSC curve of the $PLGA_{60}/PCL_{3496}$ porous scaffold under wet condition.

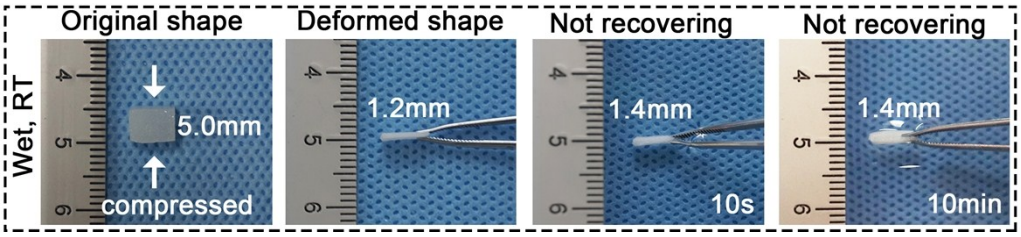

Figure S9. The stability of $PLGA_{60}/PCL_{3496}$ scaffolds under wet condition at room temperature.

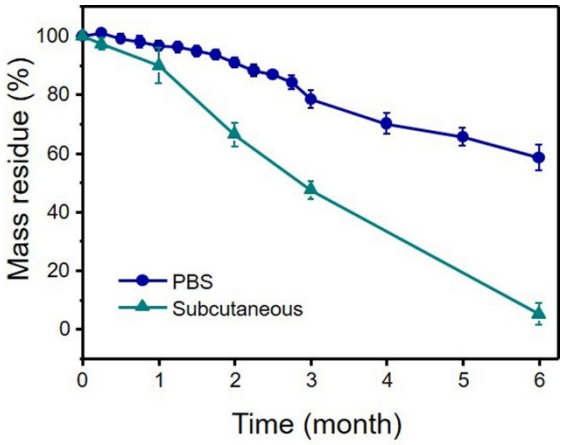

Figure S10. Degradation of $PLGA_{60}/PCL_{3496}$ porous scaffolds in PBS (0.01 M, pH = 7.4) at 37 ^{o}C and under subcutis of SD rats.

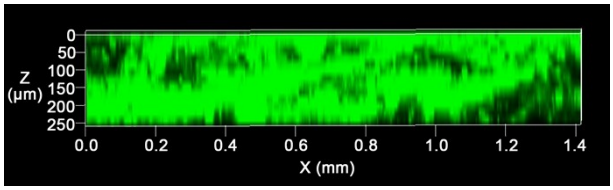

Figure S11. Confocal projection image of stem cells in a $PLGA_{60}/PCL_{3496}$ porous scaffold. **Response #1.7**

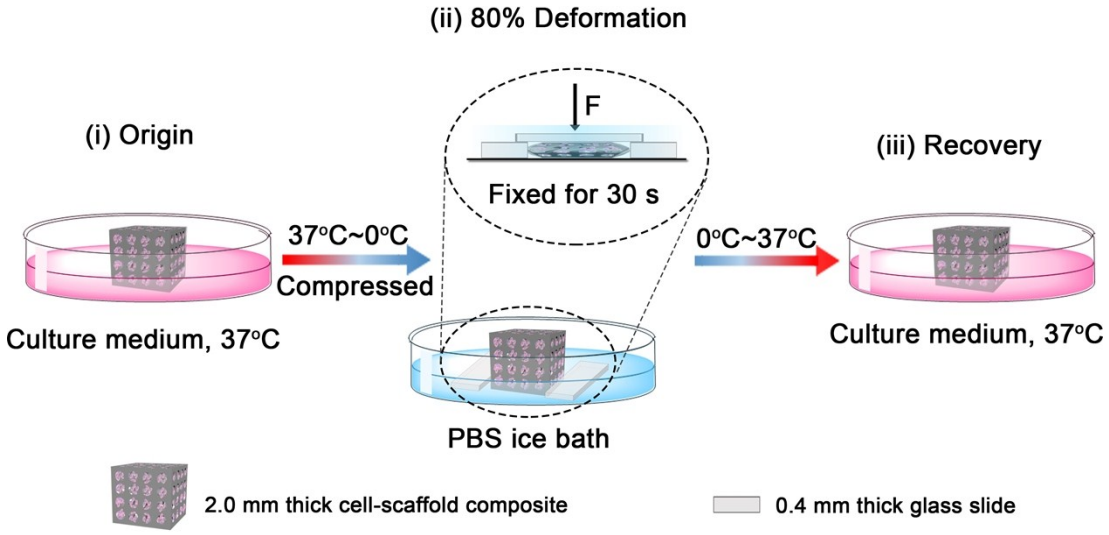

Figure S12. Experiment illustration. Stem cells were seeded on $PLGA_{60}/PCL_{3496}$ porous scaffolds at 37 °C (above T_m) and cultured for 1 day. Then, the cell-scaffold composite was compressed to 80% strain in a PBS ice bath at 0 °C (below T_c) for 30 s to fix the temporary shape. The 80% deformation was achieved by compressing the 2.0 mm thick composite to the limited height, which was determined by two 0.4 mm thick glass slides. Finally, the composite was put back to culture medium at 37 °C and recovered.

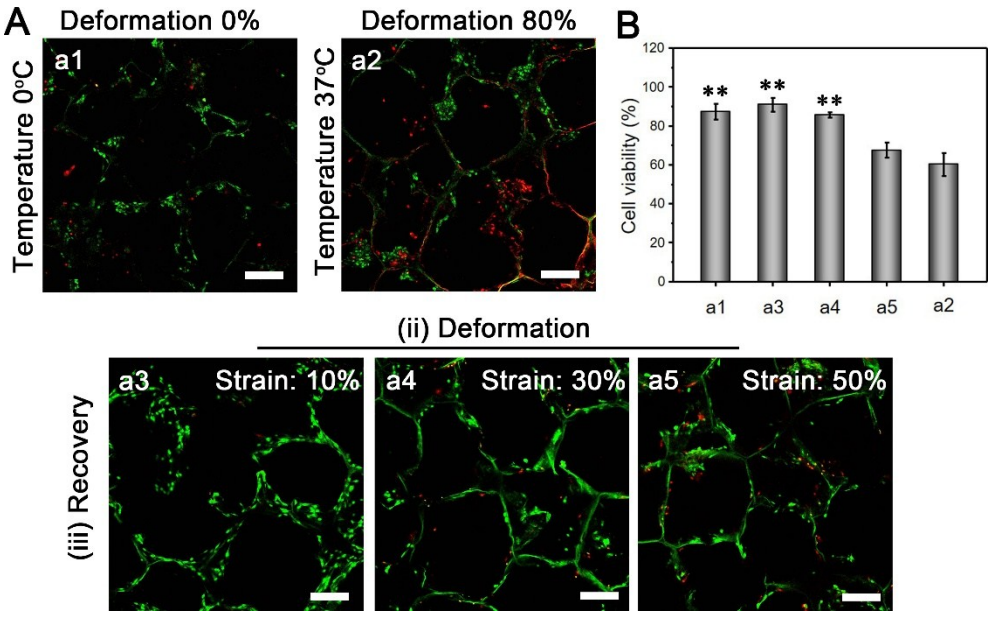

Figure S13. Cell viability under five conditions. (A) Live/dead staining images: (a1) 0 °C, 0% deformation (a2) 37 °C, 80% deformation and after shape memory with different deformation: (a3) 10%, (a4) 30%, (a5)

50%. (B) Corresponding cell viability. Scale bar is 200 μm. $^{**}P < 0.01$ compared to a5 and a2, respectively.

(**Response #1.9**)

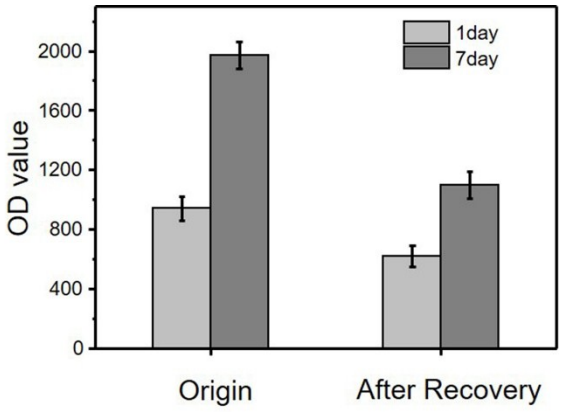

Figure S14. Cell proliferation after 1 and 7 days' culture before and after shape memory. DNA contents was detected by DNA assay using Hoechst 33258 dye and the intensity values were read on a microplate reader.

Table S1. Feed ratio of $PLGA_x/PCL_y$ porous scaffolds.

Sample ($PLGA_x/PCL_y$)	Mass (g) (PLGA:PCL)	NaCl (g)	DMSO (mL)
$PLGA_{30}/PCL_{1102}$	0.02:0.0255	7	2.2
$PLGA_{60}/PCL_{1102}$	0.02:0.0510	7	2.2
$PLGA_{90}/PCL_{1102}$	0.02:0.0769	7	2.2
$PLGA_{30}/PCL_{3496}$	0.02:0.0813	7	2.2
$PLGA_{60}/PCL_{3496}$	0.02:0.1626	7	2.2
$PLGA_{90}/PCL_{3496}$	0.02:0.2439	7	2.2
$PLGA_{30}/PCL_{7144}$	0.02:0.1662	7	2.2
$PLGA_{60}/PCL_{7144}$	0.02:0.3324	7	2.2
$PLGA_{90}/PCL_{7144}$	0.02:0.4984	7	2.2
$PLGA_{30}/PCL_{11476}$	0.02:0.2669	7	2.2
$PLGA_{60}/PCL_{11476}$	0.02:0.5338	7	2.2
$PLGA_{90}/PCL_{11476}$	0.02:0.8006	7	2.2

x: theoretical cross-link density. y: PCL-diol molecular weight.

Table S2. Primer sequences.

Target gene		Primer sequence
GAPDH	Forward	5'-ACTTTGGTATCGTGGAAGGACTCAT-3'
	Reverse	5'-GTTTTTCTAGACGGCAGGTCAGG-3'
Oct-4	Forward	5'-GAGTGAGAGGCAACCTGGAGAAT-3'
	Reverse	5'-GACCCAGCAGCCTCAAAATCC-3'
Nanog	Forward	5'-TGGATCCAGCTTGTCCCCAAA-3'
	Reverse	5'-GTGGAAGAATCAGGGCTGTCC-3'

Table S3. Characterization of PCL-diols.

M_n[a]	M_n[b]	DPI	T_c(°C)	ΔH_c(J/g)	T_m(°C)	ΔH_m(J/g)
1102	4164	1.12	17.3	75.3	35.0	81.1
3496	7553	1.16	29.6	76.5	50.9	81.0
7144	11050	1.18	33.0	71.4	55.4	76.3
11476	17304	1.21	33.9	68.7	55.8	71.1

a was obtained by ^{1}H NMR. b was obtained by GPC. PMMA was used as standard.

Table S4. Characterization of $PLGA_x/PCL_y$ porous scaffolds.

Sample	T_m (°C)	T_c (°C)	X_c (%)
$PLGA_{30}/PCL_{1102}$	–	–	–
$PLGA_{60}/PCL_{1102}$	–	–	–
$PLGA_{90}/PCL_{1102}$	–	–	–
$PLGA_{30}/PCL_{3496}$	–	–	–
$PLGA_{60}/PCL_{3496}$	38.3	1.3	22.2.
$PLGA_{90}/PCL_{3496}$	42.1	10.8	25.1
$PLGA_{30}/PCL_{7144}$	44.2	15.4	20.1
$PLGA_{60}/PCL_{7144}$	50.5	23.5	32.9
$PLGA_{90}/PCL_{7144}$	56.3	39.8	46.0
$PLGA_{30}/PCL_{11476}$	54.8	32.7	22.5
$PLGA_{60}/PCL_{11476}$	56.1	40.4	31.3
$PLGA_{90}/PCL_{11476}$	56.4	40.4	47.4

x: theoretical cross-link density. y: PCL-diol molecular weight. –: undetectable.